Synthesis and Tau RNA binding evaluation of ametantrone-containing ligands

Gerard Artigas, and Vicente Marchán*

Departament de Química Orgànica and IBUB, Universitat de Barcelona

Martí i Franquès 1-11, E-08028 Barcelona (Spain)

Fax: + (34) 93 339 7878

E-mail: vmarchan@ub.edu

TOC ABSTRACT GRAPHIC

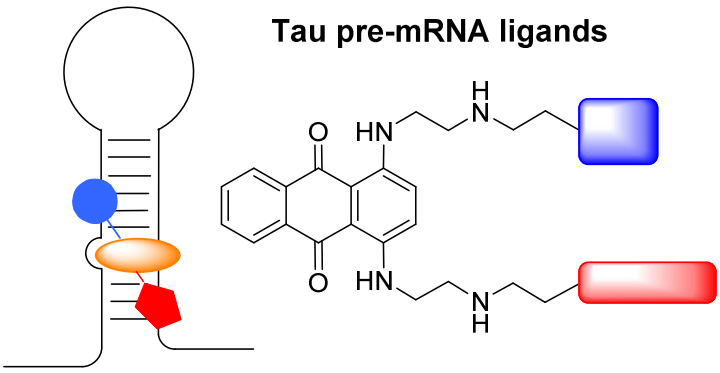

ABSTRACT

We describe the synthesis and characterization of ametantrone-containing RNA ligands based on the derivatization of this intercalator with two neamine moieties (Amt-Nea,Nea) or with one azaquinolone heterocycle and one neamine (Amt-Nea,Azq), as well as its combination with guanidinoneamine (Amt-NeaG4). Biophysical studies revealed that guanidinylation of the parent ligand (Amt-Nea) had a positive effect on the binding of the resulting compound for Tau pre-mRNA target, as well as on the stabilization upon complexation of some of the mutated RNA sequences associated with the development of tauopathies. Further studies by NMR revealed the existence of a preferred binding site in the stem-loop structure, in which ametantrone intercalates in the characteristic bulged region. Regarding doubly-functionalized ligands, binding affinity and stabilizing ability of Amt-Nea,Nea were similar to those of the guanidinylated ligand, but the two aminoglycoside fragments seem to interfere with its accommodation in a single binding site. However, Amt-Nea,Azq binds at the bulged region in a similar way than Amt-NeaG4. Overall, these results provide new insights on how fine-tuning RNA binding properties of ametantrone by single or double derivatization with other RNA recognition motifs, which could help in the future to the design of new ligands with improved selectivity for disease-causing RNA molecules.

INTRODUCTION

The search for drugs based on small molecules to control RNA function has been postulated in recent years as a promising strategy to treat human diseases.[1] This is supported by the great biological relevance of both coding and non-coding RNA molecules,[2] and by the fact that only a small number of the proteins linked to genetic diseases can be targetable with drug-like compounds.[3] In addition, the folding of local secondary structures of therapeutically relevant RNA targets into complex three dimensional architectures offers the possibility, like in proteins, of using ligands for targeting specific binding sites in a selective manner.[4] However, despite the great potential of RNA as a drug target, finding selective ligands for a specific sequence and with drug-like properties still remains a challenge. The high conformational dynamics of this biomolecule together with our limited understanding of ligand-RNA recognition principles difficult the *de novo* design of selective RNA ligands.[5] Within this scenario, the modification of known building blocks by using fragment-based approaches[6] offers an alternative for developing compounds with improved RNA-binding properties (e.g. affinity, sequence specificity and cellular permeability), as well as for gaining knowledge on RNA recognition mechanisms. Among the large number of RNA ligands described in the literature so far, the anticancer drug mitoxantrone (Mtx in Scheme 1) has received attention recently. This classical nucleic acid intercalator was identified in a high-throughput screening as a promising ligand[7] of the RNA secondary structure located at the exon 10-5' intron junction of Tau pre-mRNA, which is involved in the regulation of the alternative splicing of tau protein.[8] According to NMR structural data,[7b] this compound intercalates between the two G:C pairs flanking the bulged adenine in the stem-loop structure of Tau. In addition, the two side arms of the anthraquinone moiety play an important role in the recognition of this characteristic binding site. Mitoxantrone also binds HIV-

1 transactivation response element (TAR) RNA with nM affinity, although non-specific binding was also found in competition assays with tRNA.[9]

Taking into account our previous results on Tau RNA ligands based on the combination of acridines with the small aminoglycoside neamine,[10] we recently focused on a derivative of mitoxantrone lacking the phenolic hydroxyl groups. This heteroaromatic compound, known as ametantrone (Amt in Scheme 1), was selected because of its proven reduced cytotoxicity in eukaryotic cells compared with mitoxantrone.[11] Dynamic combinatorial chemistry together with biophysical experiments demonstrated that the combination of ametantrone with neamine led to ligands with high binding affinity (nM scale for Tau RNA), particularly when both moieties were conjugated through a short spacer (Amt-Nea in Scheme 1).[12] NMR spectroscopic studies of the complex between this compound and Tau RNA revealed the existence of a preferred binding site in which ametantrone intercalates in the bulged region of the stem-loop structure and the neamine moiety and the Amt side chains interact with the major groove of the RNA. Importantly, Amt-Nea was able to increase the thermodynamic stability of Tau RNA mutated sequences involved in the onset of frontotemporal dementia with parkinsonism linked to chromosome 17 (FTDP-17)[8] to a similar or even higher levels than that of the wild-type sequence. The stabilization of Tau RNA mutated sequences upon ligand complexation could be used to modulate Tau pre-mRNA splicing and, for instance, to counteract the negative effects of dementia-causing mutations.[7,8] Moreover, the presence of the characteristic bulged adenine nucleotide flanked by G:C pairs in other therapeutically relevant RNA targets, such as the Rev response element (RRE) RNA, opens the door to the development of selective ligands for this RNA motif based on Mtx/Amt derivatives.[13]

On the basis of all these precedents, we wondered how derivatization of the free side arm of the anthraquinone moiety in Amt-Nea (Scheme 1) could affect its Tau RNA-binding properties, particularly binding affinity and stabilizing ability against FTDP-17-causing mutations, as well as

to assess if the preferred binding site at the bulged region is maintained. Here we report the synthesis and Tau RNA binding studies of ligands (Scheme 1) based on the derivatization of ametantrone with two neamine moieties (Amt-Nea,Nea) or with one neamine and one azaquinolone (Amt-Nea,Azq). The azaquinolone moiety was selected because of the potential of this heteroaromatic compound to recognize the bulged adenine in the stem-loop via complementary hydrogen bonding pairing.[14] The guanidinylated analogue of Amt-Nea (named Amt-NeaG4) was also included in this study, since guanidinylation has proved to be a promising approach to improve RNA-binding properties of aminoglycoside-containing compounds as well as their cellular uptake.[10b,15]

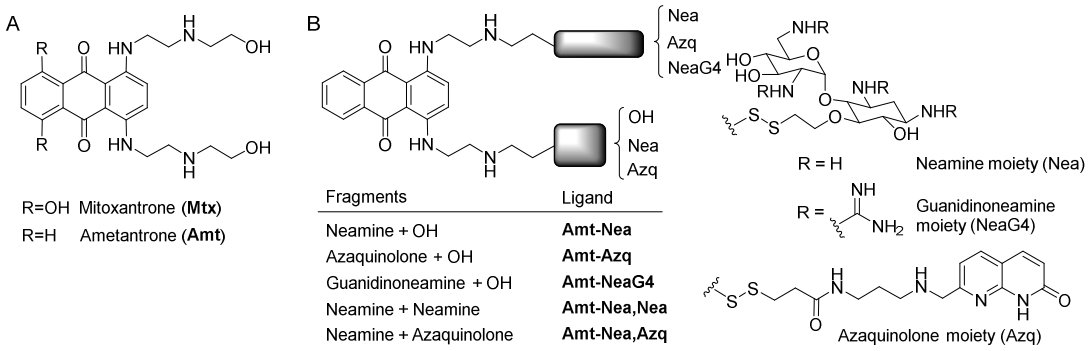

Scheme 1. (A) Structure of mitoxantrone and ametantrone. (B) Schematic representation of ligands based on the derivatization of ametantrone through one or the two side chains of the anthraquinone ring.

RESULTS AND DISCUSSION

Synthesis of Amt-containing ligands.

The synthesis of second generation ametantrone-containing ligands (Amt-NeaG4, Amt-Nea,Nea and Amt-Nea,Azq; Scheme 1) was planned in solution by using thiol-disulfide exchange reactions mediated by 2,2′-dithiobis-(5-nitropyridine) (DTNP).[12,15,16] For this purpose, two ametantrone derivatives were prepared in which one or the two hydroxyl groups of the side chains of the anthraquinone heterocycle were replaced by thiol functions masked as thioacetyl (**2** and **3**, respectively, see Scheme 2). First, reaction of 1,4-difluoroanthraquinone with an excess of *N*-(2-hydroxyethyl)ethylenediamine afforded ametantrone, whose secondary alkyl amino functions were selectively Boc protected to afford intermediate **1**.[12] After Mitsunobu reaction with DIAD, PPh_3 and thiolacetic acid, the *mono*- (**2**, 36%) and *bis*-thioacetyl (**3**, 59%) derivatives were isolated by silica column chromatography and fully characterized by NMR and MS.

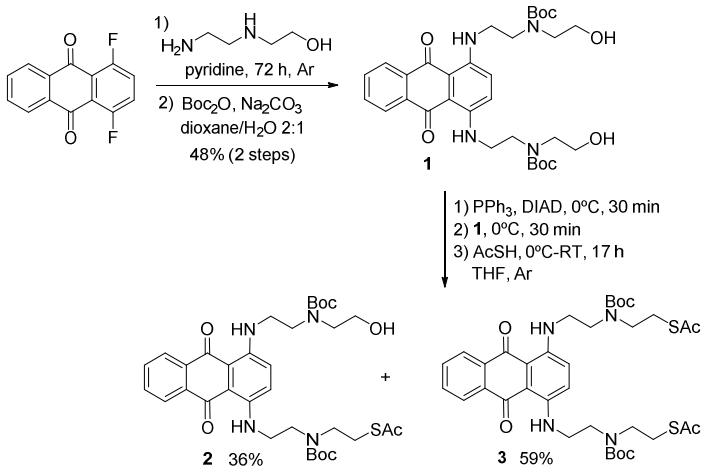

Scheme 2. Synthesis of Boc-protected ametantrone derivatives **2** and **3**.

For the synthesis of the guanidinylated analogue of Amt-Nea, we used *N*,*N*′-di-Boc-*N*″-triflylguanidine, since we and others have demonstrated previously the utility of this reagent to

transform amino groups into guanidinium in compounds incorporating aminoglycoside fragments such as neamine or neomycin.[10b,15,17] To avoid possible side-reactions with the two alkyl secondary amino functions of the anthraquinone moiety during guanidinylation, we decided to keep them masked with the Boc group (Scheme 3). First, the thiol-containing neamine derivative **4**[10] was activated with DTNP under acidic conditions overnight under an Ar atmosphere. Reaction of intermediate **5** with the thiol derivative of *bis*-Boc-protected ametantrone **6,**[12] which was easily prepared by hydrolysis of the thioester group of **2** with sodium methoxide, afforded the expected disulfide intermediate **7** after purification by reversed-phase HPLC. Finally, reaction of **7** with *N*,*N′*-di-Boc-*N″*-triflylguanidine in the presence of triethylamine followed by acidic deprotection with a TFA cocktail containing triisopropylsilane as cation scavenger, afforded the trifluoroacetate salt of the desired compound as a dark blue solid after purification by HPLC and lyophilisation (yield 64%). **Amt-NeaG4** was fully characterized by NMR (1D ^{1}H, COSY, TOCSY) and high-resolution ESI mass spectrometry. Despite the prolonged reaction time (14 days) and the use of a large excess of the guanidinylating reagent (up to 360-fold molar equivalent), the triguanidinylated derivative was also identified in the reaction crude (see Figure S1 in the Supporting Information), which can be attributed to the steric hindrance caused by the Boc groups in the anthraquinone moiety.

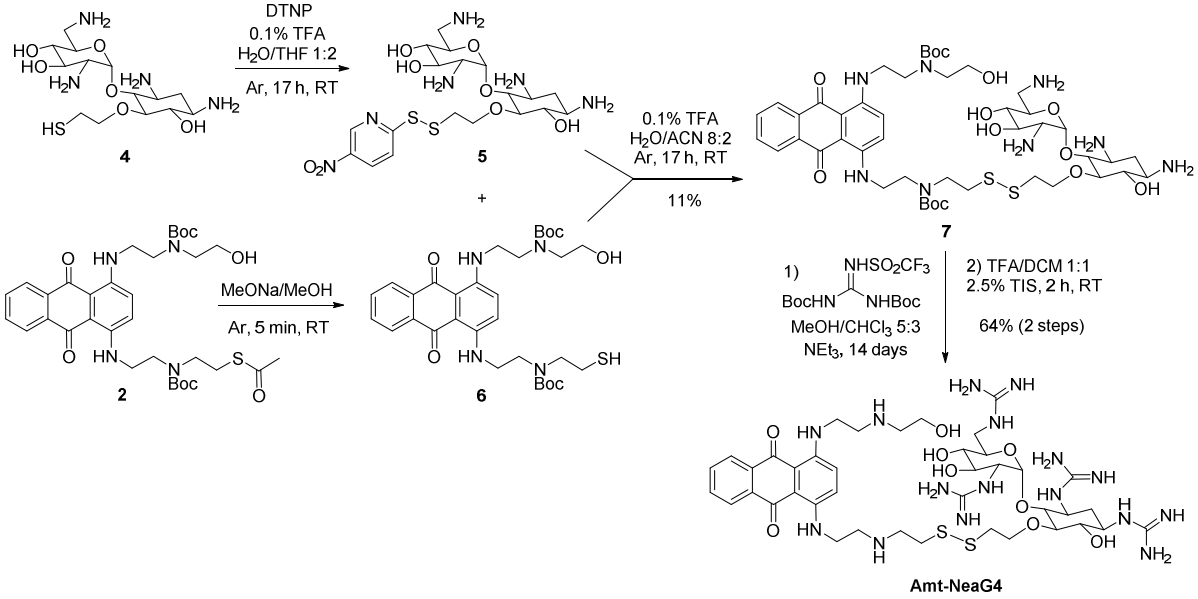

Scheme 3. Synthesis of the guanidinylated ligand **Amt-NeaG4**.

As shown in Scheme 4, a similar approach was used for the synthesis of doubly-functionalized amentantrone-containing ligands. In this case, the Boc protected derivative of ametantrone containing one thioacetyl group at each side chain was used (**3**). After hydrolysis of the two thioester groups with sodium methoxide, the thiol derivative **8** was reacted with an excess of the activated neamine **4** under slightly acidic conditions during 5 days at room temperature. The Boc-protected intermediate, Amt(Boc)$_2$-Nea,Nea was treated with TFA/TIS/H_2O 95:2.5:2.5 for 1 h at room temperature and the expected ligand, Amt-Nea,Nea, was isolated by HPLC with an overall 6% yield. Regarding the synthesis of the compound containing three different RNA-binding moieties, the thiol-containing ametantrone derivative **8** was reacted simultaneously with activated neamine (**5**) and activated azaquinolone (**9**)[12] derivatives. After TFA treatment, Amt-Nea,Azq was isolated by HPLC and characterized by MS and NMR (overall yield 8%). The formation of several side-products (e.g. Amt-Nea,Nea and Amt-Azq,Azq during the synthesis of Amt-

Nea,Azq) due to lack of selectivity during the formation of disulfide bonds accounts for the low yield in both cases (see HPLC traces of the crudes in Figure S1 in the Supporting Information).

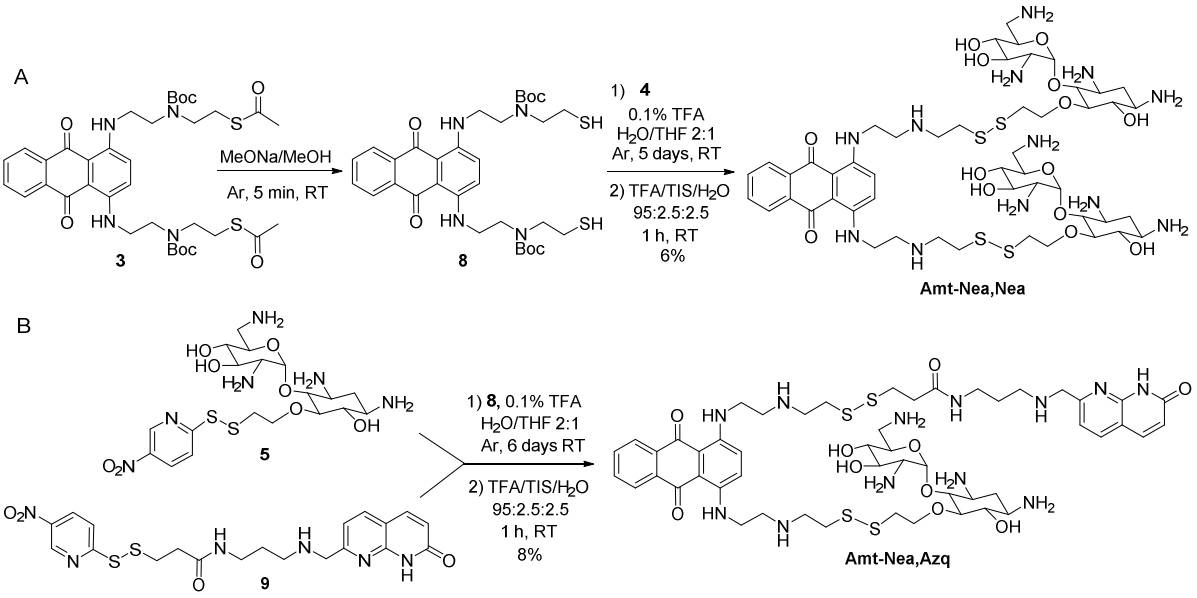

Scheme 4. Synthesis of the doubly-functionalized ligands, **Amt-Nea,Nea** (A) and **Amt-Nea,Azq** (B).

Biophysical studies on the interaction of Amt-containing ligands with Tau RNA.

Our next objective was to study the interaction of the new ametantrone-containing ligands (Amt-NeaG4 , Amt-Nea,Nea and Amt-Nea,Azq) with Tau RNA, and in particular to assess how the modifications introduced in the parent Amt-Nea ligand (e.g. guanidinylation or double functionalization) influence RNA binding affinity as well as their ability to stabilize the disease-causing mutated sequences.[8] First, quantitative binding studies were carried out by fluorescence titration experiments by using 5'-end fluorescein-labelled wt RNA. As shown in Figure 1, the oligoribonucleotide fluorescence was quenched upon addition of increasing concentrations of the ligands, which reproduce the tendency previously found with other Tau RNA ligands containing heteroaromatic moieties.[7b,10,12] A characteristic dose-dependent curve was obtained when the normalized fluorescence was plotted in front of the compound concentration. The inherent

fluorescence of the ligands was always subtracted from that of the labelled RNA by repeating the full titration in the absence of RNA. This approach allows the determination of EC_{50} values (the effective ligand concentration required for 50% RNA response) by fitting the data to a sigmoidal dose-response curve (Figure 1).

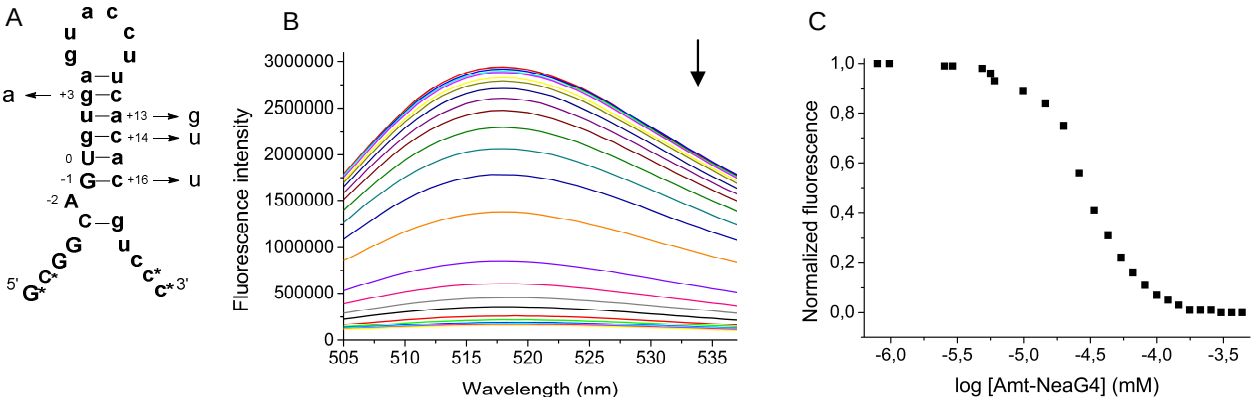

Figure 1. (A) Sequences and secondary structure of wild-type (wt) and of some mutated Tau stem-loop RNAs (+3, +13, +14 and +16). Exonic sequences are shown in capital letters and intronic sequences in lower case. Nucleotides involved in base pairs, previously identified by NMR, are connected by a dash.[7b,8b] An asterisk denotes 2'-*O*-methyl modification. In fluorescence binding experiments, fluorescein derivatization was performed at the 5' end. (B) Fluorescence quenching of wt Tau RNA labelled with fluorescein upon addition of increasing concentrations of Amt-NeaG4. Experimental conditions: [RNA] = 25 nM and [ligand] = 0 to 614 nM, in 10 mM sodium phosphate buffer pH 6.8, 100 mM NaCl and 0.1 mM Na_2EDTA. (C) Plot of the normalized fluorescence signal at 517 nm against the log of the ligand concentration. The normalized fluorescence was calculated by dividing the difference between the observed fluorescence, *F'*, and the final fluorescence, F_f, by the difference between the initial fluorescence, F_0, and the final fluorescence, F_f.

The EC_{50} values of the new ametantrone-containing ligands together with those of ametantrone, mitoxantrone, neamine and guanidinoneamine are shown in Table 1. EC_{50} values of the Amt-Nea and Amt-Azq ligands have also been included for comparison purposes.[12] Consistent with our previous results,[10b,15] the guanidinylation of the neamine moiety had a positive effect on the binding affinity of Amt-Nea. Indeed, the EC_{50} value for Amt-NeaG4 was about 1.2 times lower than for the parent amino ligand (e.g. EC_{50} = 57.2 $\pm$ 2.0 nM for Amt-NeaG4 *vs.* EC_{50} = 70.6 $\pm$ 7.2 nM for Amt-Nea). The opposite tendency was found when a second fragment (neamine or azaquinolone) was incorporated in the free side chain of ametantrone in Amt-Nea: the EC_{50} values for Amt-Nea,Nea and for Amt-Nea,Azq were 1.1 and 1.2 times higher than for Amt-Nea, respectively. However, it is worth noting that the affinity of both doubly-functionalized ligands is still higher higher than that of ametantrone, thereby suggesting that, upon ligand complexation, the two RNA binding moieties attached to the anthraquinone intercalator might participate in the interaction with the RNA target.

Fluorescence binding assays were repeated in the presence of a biologically relevant competitor (a $tRNA^{mix}$ from baker's yeast) to get some insights on their specificity for Tau RNA. As shown in Table 1, the specificity of the ligands was highly dependent on the nature of the modification introduced in the parent ligand. In the presence of the competitor, the EC_{50} value of Amt-NeaG4 for Tau RNA was increased by 10-fold, whereas those of Amt-Nea,Nea and Amt-Nea,Azq were increased by about 7-fold. Hence, guanidinylation of the neamine moiety in Amt-Nea seems to have a negative effect on the specificity compared with the introduction of a second RNA binding moiety. The fact that all ametantrone ligands containing one or two neamine moieties or guanidinoneamine are less specific than the parent anthraquinone building blocks (Mtx or Amt) or Amt-Azq is in agreement with the known promiscuity of aminoglycosides and their derivatives.

Table 1. Binding of the ligands to wt RNA in the absence or in the presence of a tRNA competitor.

Ligand	EC_{50} (nM)[a]	EC_{50} (nM) +tRNA[b]	EC_{50}+tRNA / EC_{50}
Neamine	$3.1x10^6$	nd	nd
Guanidinoneamine	830	nd	nd
Mitoxantrone	168.8 ± 6.2	803.3	4.8
Ametantrone	231.8 ± 8.0	675.6	2.9
Amt-Azq[c]	162.5 ± 5.7	570.7	3.5
Amt-Nea[c]	70.6 ± 7.2	569.8	8.1
Amt-NeaG4	57.2 ± 2.0	580.1	10.2
Amt-Nea,Nea	76.2 ± 4.1	519.7	6.8
Amt-Nea,Azq	84.5 ± 3.8	558.6	6.6

[a]All fluorescence measurements were performed in 10 mM sodium phosphate buffer pH 6.8, 100 mM NaCl and 0.1 mM Na_2EDTA. [b]Measured in the presence of a 30-fold nucleotide excess of a mixture of tRNA ($tRNA^{mix}$). [c]EC_{50} values of these ligands[12] have been included in the table for comparison purposes.

Next, we investigated the ability of second generation Amt-containing ligands to stabilize Tau RNA, in particular some of the mutated sequences found in patients suffering from tauopathies like FTDP-17. These intronic mutations (denoted as +3, +13, +14 and +16 in Figure 1) are known to decrease the thermodynamic stability of the stem-loop structure located at the exon 10-5' intron junction of Tau pre-mRNA.[8] As previously stated, reversing the destabilization of these mutated sequences upon ligand complexation has been postulated as a therapeutic tool to restore the physiological balance of tau isoforms generated upon abnormal alternative splicing and, for instance, as a potential treatment for such neurodegenerative diseases.

UV melting experiments were carried out by monitoring the absorbance as a function of temperature. The midpoint of the transition (see Figures S2-S5 in the Supporting Information) is referred to as the melting temperature (T_m), and provides an indicative of the thermal stability of the RNA secondary structure in the presence of a given ligand. As shown in Table 2, guanidinylation of Amt-Nea had a positive effect on the thermal stability of wt RNA upon complexation (ΔT_mG = +3.1^oC; ΔT_mG indicates the effect of guanidinylation compared with that of the parent non-guanidinylated ligand, Amt-Nea). This effect was similar with the +14 mutated sequence (ΔT_mG = +2.4^oC) but slightly lower with the +16 mutant (ΔT_mG = +0.7^oC). However, the stabilizing effect of Amt-NeaG4 upon complexation with the +3 mutated RNA (ΔT_mG = -1.3^oC) was lower than in the presence of Amt-Nea, but still substantially higher (ΔT_m = +11.6^oC) compared with that of Amt (ΔT_m = +2.8^oC) or Mtx (ΔT_m = +5.7^oC) with this mutated sequence. Regarding doubly-functionalized ligands, the tendency was found to be the opposite depending on the nature of the second moiety attached to the anthraquinone fragment in the Amt-Nea ligand, neamine or azaquinolone. As shown in Table 2, the effect of Amt-Nea,Nea on the thermal stability of all RNA sequences was always higher than that of the parent ligand. This increase was particularly high for the wt (ΔT_m = +8.9^oC with Amt-Nea *vs.* ΔT_m = +13^oC with Amt-Nea,Nea) and the +14 mutant (ΔT_m = +10.4^oC with Amt-Nea *vs.* ΔT_m = +14.4^oC with Amt-Nea,Nea). However, the stabilization induced by Amt-Nea,Azq was considerably lower than that of Amt-Nea. Such differences were particularly important with wt RNA (ΔT_m = +8.9^oC with Amt-Nea *vs.* ΔT_m = +4.7^oC with Amt-Nea,Azq) and with the +3 mutated sequence (ΔT_m = +12.9^oC with Amt-Nea *vs.* ΔT_m = +6.8^oC with Amt-Nea,Azq). These results are quite surprising because EC_{50} values of Amt-Nea,Nea and Amt-Nea,Azq point to similar binding affinities for Tau RNA. Despite this reduced stabilizing ability, the neamine moiety in Amt-Nea,Azq still

seems to have a positive effect on the thermal stabilization of the RNAs upon complexation, as inferred from the higher T_m values of its complexes compared with those obtained in the presence of Amt-Azq

Table 2. Melting temperatures (T_m) for the complexation of the ligands with Tau RNAs (1 µM both in RNA and in ligands in 10 mM sodium phosphate buffer, pH 6.8, 100 mM NaCl and 0.1 mM Na_2EDTA).

	T_m wt	ΔT_m [a]	T_m	ΔT_m [a]	T_m	ΔT_m [a]	T_m	ΔT_m [a]
No ligand	66.5	-	51.4	-	53.5	-	59.6	
Neamine	66.9	+0.4	51.5	+0.1	54.0	+0.5	60.1	+0.5
Guanidinoneamine	67.7	+1.2	52.8	+1.4	54.5	+1.0	61.0	+1.4
Mitoxantrone	69.2	+2.7	57.1	+5.7	58.1	+4.6	63.4	+3.8
Ametantrone	67.1	+0.5	54.2	+2.8	55.7	+2.2	61.6	+2.0
Amt-Azq	67.8	+1.3	56.1	+4.7	57.3	+3.8	61.8	+2.2
Amt-Nea	75.4	+8.9	64.3	+12.9	63.9	+10.4	69.4	+9.8
Amt-NeaG4	78.5	+12.0	63.0	+11.6	66.3	+12.8	70.1	+10.5
Amt-Nea,Nea	79.5	+13.0	67.0	+15.6	67.9	+14.4	70.8	+11.2
Amt-Nea,Azq	71.2	+4.7	58.2	+6.8	61.1	+7.6	66.3	+6.7

[a] ΔT_m= (T_m of the RNA in the presence of ligand) – (T_m of RNA alone).

Spectroscopic studies on the interaction of Amt-containing ligands with Tau RNA.

The overall biophysical studies indicated that both binding affinity and stabilizing ability of the parent Amt-Nea ligand are influenced either by guanidinylation of the aminoglycoside moiety or by functionalization of the second arm of ametantrone. Hence, our next objective was focused on investigating the effect of these ligands (Amt-NeaG4, Amt-Nea,Nea and Amt-Nea,Azq) on the structure of Tau RNA upon complexation, and in particular to determine if they also have a

preferred binding site. As previously stated, intercalation of the anthraquinone moiety in the bulged region of the stem-loop structure of Tau RNA together with specific contacts between the positively-charged side chains and the neamine moiety with the RNA, account for the high binding affinity and stabilizing ability of Amt-Nea.[12]

First, fluorescence emission spectra (upon excitation at 547 nm) were recorded for the three compounds in the absence and in the presence of increasing amounts of wt Tau RNA. As shown in Figure 2, hypochromic and bathochromic effects were observed in the fluorescence spectra of the ligands during the titration with RNA, although those effects were more pronounced in the case of Amt-NeaG4 and Amt-Nea,Nea, which is consistent with a higher binding affinity. Interestingly, a strong hypochromism was observed in the fluorescence spectra of these ligands in the first stage of the titration (0.07 mol equiv. of RNA for Amt-NeaG4 and 0.17 mol equiv. of RNA for Amt-Nea,Nea). Then, in the second stage of the titration, the intensity of the fluorescence emission band increased gradually until saturation was reached, and then decreased again. In both cases, an 8 nm shift to higher wavelengths was observed (from the initial 656 nm band in the free ligand). These results reproduced those previously observed for mitoxantrone[8b] and for the parent Amt-Nea ligand,[12] and suggest that neither guanidinylation nor double functionalization of ametantrone with two neamine moieties seem to difficult the intercalation of the anthraquinone fragment. Although this two-stage binding mode was not completely reproduced in the case of Amt–Nea,Azq, which could be attributed to a lower binding affinity compared with that of the Amt-NeaG4 or Amt-Nea,Nea, the quenching of the fluorescence intensity points also to the intercalation of the ametantrone fragment.

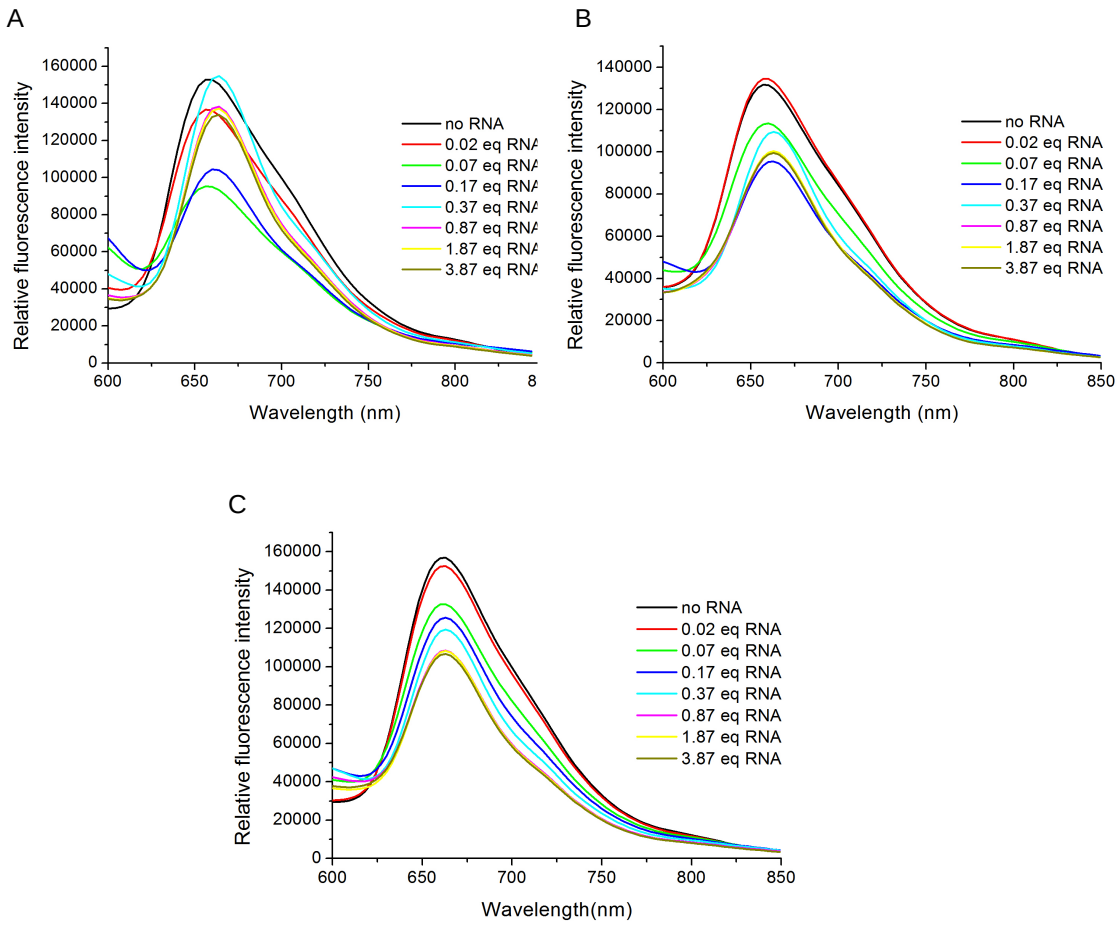

Figure 2. Fluorescence emission spectra of Amt-NeaG4 (A), Amt-Nea,Nea (B) and Amt-Nea,Azq (C) in the absence and in the presence of increasing amounts of wt RNA in a 10 mM sodium phosphate buffer, pH 6.8, containing 100 mM NaCl and 0.1 mM Na_2EDTA. 2 µM solutions of the ligands were used in fluorescence titration experiments. The emission spectra were recorded from 600 ~ 850 nm with λ_{ex} = 547 nm.

Although qualitative information on the interaction of heteroaromatic compounds with nucleic acids can be obtained from UV-Vis or fluorescence spectroscopy,[18] these techniques do not provide detailed structural information on their binding mode, which is necessary to rationalize their RNA-binding properties and, more importantly, to help in the design of more selective ligands with improved ones. In this context, NMR spectroscopy is a powerful technique to detect

RNA-ligand interactions, particularly in the case of ligands based on the combination of fragments.[19]

Titration experiments of Tau RNA with ametantrone-containing ligands (Amt-NeaG4, Amt-Nea,Nea and Amt-Nea,Azq) were monitored by NMR spectroscopy (see Figure 3 and Figure S6 in the Supporting Information) to get more detailed information on their mode of interaction. Interestingly, a similar behaviour to that previously found with the parent ligand Amt-Nea[12] was observed upon addition of either Amt-NeaG4 or Amt-Nea,Azq (see the exchangeable proton region of the NMR spectra in Figure 3), including little line broadening and changes in the chemical shifts of some imino protons of the RNA close to the bulged region. The co-existence of imino signals arising from the free and bound RNA at a RNA:ligand ratio of 1:0.5 indicates that both species are in slow equilibrium in the NMR time scale. Moreover, the fact that only one set of signals at a 1:1 ratio was observed suggests that Amt-NeaG4 and Amt-Nea,Azq bind Tau RNA in a well defined binding site. As shown in Figure 3, imino signals of the complex between Tau RNA and the ligands at a 1:1 ratio were labelled according to previously reported data from the complex Tau-Amt-Nea due to their similar behaviour during the titration.[12] In both cases, the most pronounced changes in chemical shifts involved the imino proton of G-1 (see Figure 3 for the labelling of the imino protons), which was shifted by about –0.85 ppm upon complexation with Amt-NeG4 or Amt-Nea,Azq, compared with their values in the free RNA. In contrast, the effect of Amt-Nea,Azq on the imino signal of U0 was much higher than that provoked by Amt-NeaG4 (+0.35 and +0.13 ppm, respectively), and in both cases imino signals of G+1, U+2 and G+3 were not significantly affected in the complexes. As previously found with Amt-Nea, appearance of an imino signal which was assigned to G+17 confirms the allocation of both ligands at the bulged region of the stem-loop structure, particularly of the amentatrone fragment which would protect the C-3:G+17 base pair from the solvent in the complex. In addition, the two

signals in the exchangeable proton region ($\delta \approx 9.9$ and 9.5 ppm) corresponding to the aliphatic amino protons of the two side chains of the ametantrone moiety of the ligand were clearly observed upon complexation with Amt-NeaG4 or Amt-Nea,Azq, suggesting again a similar binding mode to that described for Amt-Nea.[12]

To our surprise, addition of Amt-Nea,Nea caused a general line broadening of all signals together with major changes in the chemical shifts of the imino protons of the RNA (see Figure 3). The fact that two set of signals corresponding to the aliphatic amino protons of the ametantrone moiety of the ligand were observed upon complexation ($\delta \approx 9.9$ and 9.4 ppm, and $\delta \approx 10.5$ and 10.6 ppm) suggests the presence of two binding sites for this ligand in Tau RNA. Hence, besides allocation at the bulged region of Tau RNA, the presence of two neamine fragments seems to direct the binding of Amt-Nea,Nea to another region of the stem-loop structure, probably at the loop or at the major groove. In addition, the large number of signals at the imino proton region also suggests weak aggregation as a consequence of the complexation of Tau RNA with Amt-Nea,Nea.

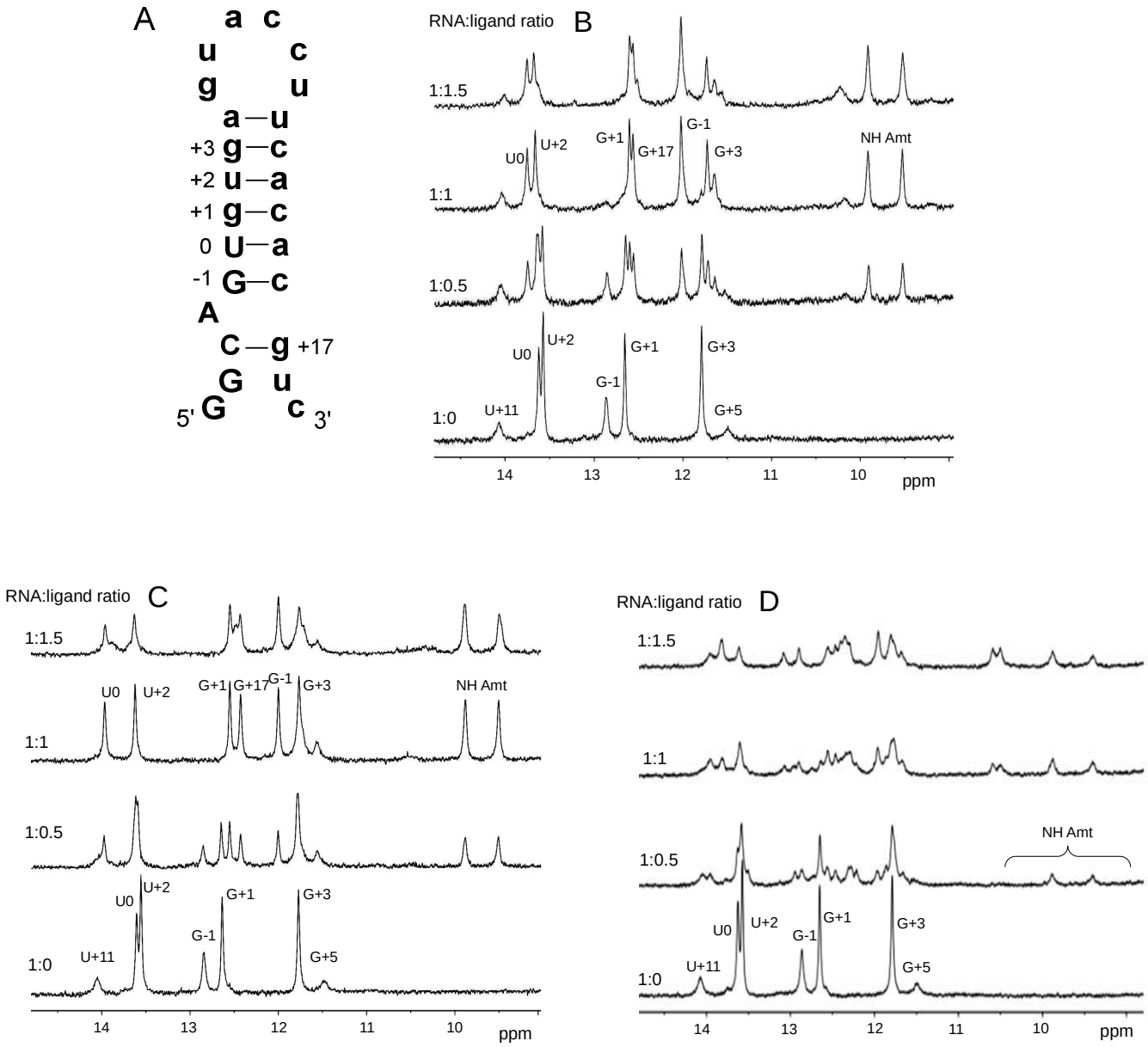

Figure 3. Secondary structure of wt Tau RNA sequence showing the labelling of the characteristic imino signals (A) and imino region of the NMR spectra of the oligoribonucleotide alone and in the presence of increasing amounts of the ligands, Amt-NeaG4 (B), Amt-Nea,Azq (C) or Amt-Nea,Nea (D). From bottom to top: ligand/RNA ratio = 0.0, 0.5, 1.0 and 1.5. Assignments for the RNA alone are labelled according to previously reported works.[7b,8b,12] Imino signals at RNA/ligand ratio 1:1 are labelled according to the

complex between Tau RNA and Amt-Nea.[12] Experimental conditions: [RNA]= 70 μM, 10 mM phosphate buffer in H_2O/D_2O 90:10, pH= 6.8, T=5ºC.

CONCLUSIONS

In summary, in this work we have described two new Tau RNA ligands based on the derivatization of ametantrone with two neamine moieties (Amt-Nea,Nea) or with one azaquinolone heterocycle and one neamine moiety (Amt-Nea,Azq), with the aim of exploring how functionalization of the two side chains of this anthraquinone intercalator affects RNA-binding properties. A guanidinylated ligand based on the derivatization of ametantrone with a single guanidinoneamine moiety (Amt-NeaG4) was also synthesized. Biophysical studies have demonstrated that these compounds bind Tau RNA with high affinity, particularly the guanidinylated derivative (EC_{50} = 57.2 nM), and that the double functionalization of ametantrone does not conduce to a significant decrease in their binding affinity (only about 1.1-1.2 fold) when compared with the parent ligand (Amt-Nea). In addition, all the compounds cause a significant increase in the thermal stability of Tau RNA, particularly Amt-NeaG4 and Amt-Nea,Nea (ΔT_m =+12 and +13 ºC, respectively). Interestingly, these compounds are able to restore the thermodynamic stability of some of the mutated sequences associated with the development of FTDP-17 disease to a higher level than that of wt RNA, which is of high relevance for developing potential modulators of Tau pre-mRNA splicing. For example, the T_m value of the +16 mutated sequence when complexed with these ligands was about 4ºC higher than that of wt RNA alone. Finally, NMR titration experiments revealed that Amt-NeaG4 and Amt-Nea,Azq have a preferred binding site in the stem-loop structure of Tau RNA, in which ametantrone intercalates in the bulged region, thereby indicating that conjugation with guanidinoneamine or with neamine and azaquinolone does not seem to modify the preference of this anthraquinone

derivative for this region. Although attachment of two aminoglycoside moieties conduce to a ligand with promising RNA-binding properties, the lack of a preferred binding site in the RNA target discards Amt-Nea,Nea as a lead compound for further developing RNA ligands for regulating the alternative splicing of Tau pre-mRNA. All together the present work reported here provides new insights for designing ligands based on amentantrone with improved RNA-binding properties. Current efforts are aimed at exploring the use of these and other amentantrone-containing derivatives as ligands of other therapeutically relevant RNA secondary structures involved in the onset of human diseases.

EXPERIMENTAL SECTION

Materials and Methods. Unless otherwise stated, common chemicals and solvents (HPLC grade or reagent grade quality) were purchased from commercial sources and used without further purification. Aluminium plates coated with a 0.2 mm thick layer of silica gel 60 F_{254} were used for thin-layer chromatography analyses (TLC), whereas flash column chromatography purification was carried out using silica gel 60 (230-400 mesh).

Reversed-phase high-performance liquid chromatography (HPLC) analyses of the ligands and their precursors were carried out on a Jupiter Proteo C_{18} column (250x4.6 mm, 90 Å 4 μm, flow rate: 1 mL/min) using linear gradients of 0.045% TFA in H_2O (A) and 0.036% TFA in ACN (B). In some cases, purification was carried out using the same analytical column. A semipreparative Jupiter Proteo column was used for the purification of some compounds (250x10 mm, 90 Å 10 μm, flow rate: 3 mL/min), using linear gradients of 0.1% TFA in H_2O (A) and 0.1% TFA in ACN (B).

NMR spectra were recorded at 25ºC in a 600 MHz spectrometer using deuterated solvents. The residual signal of the solvent was used as a reference in ^{1}H spectra. Chemical shifts are reported in part per million (ppm) in the δ scale, coupling constants in Hz and multiplicity as follows: s (singlet), d (doublet), t (triplet), q (quadruplet), qt (quintuplet), m (multiplet), dd (doublet of doublets), td (doublet of triplets), ddd (doublet of doublet of doublets), br (broad signal). High-resolution matrix-assisted laser desorption ionization time-of-flight (MALDI-TOF) mass spectra were recorded both in positive (2,4-dihydroxybenzoic acid matrix) or negative mode (2,4,6-trihydroxyacetophenone matrix with ammonium citrate as an additive). Electrospray ionization mass spectra (ESI-MS) were recorded on an instrument equipped with single quadrupole detector coupled to an HPLC, and high-resolution (HR) ESI-MS on LC/MS-TOF instrument.

Oligoribonucleotides were synthesized on a DNA automatic synthesizer (1-μmol scale) using 2'-*O*-*tert*-butyldimethylsilyl protection and following standard procedures (phosphite triester approach). RNA and fluorescein phosphoramidites, solid-supports, reagents and solvents for oligoribonucleotide synthesis were purchased from Glen Research or Link Technologies. RNase-free reagents, solutions and materials were used when manipulating oligoribonucleotides. RNase-free water was obtained directly from a Milli-Q system equipped with a 5000-Da ultrafiltration cartridge.

Reversed-phase HPLC was used for the analysis and purification of the oligoribonucleotides using linear gradients of 0.1 M aqueous NH_4HCO_3, and a 1:1 mixture of 0.1 M aqueous NH_4HCO_3 and ACN. A Kromasil C_{18} column (250x4.6 mm, 10 μm, flow rate: 1 mL/min) was used for RNA analysis whereas a semipreparative Jupiter C_{18} column (250x10 mm, 300 Å 10

μm, flow rate: 3 mL/min) was used for purification at large scale. Characterization was carried out by high resolution MALDI-TOF MS (negative mode, THAP matrix with ammonium citrate).

Synthesis of ametantrone-containing ligands.

Amt-NeaG4. First, 2,2'-dithiobis(5-nitropyridine) (11.6 mg, 37.5 μmol) and the neamine thiol monomer **4** (3 μmol) were reacted in a 2:1 (v/v) mixture of THF/aqueous 0.1 % TFA (2 mL) under argon at RT. After 17 h, THF was evaporated *in vacuo* and the remaining yellow solution was diluted with H_2O (2 mL). The aqueous phase was washed with AcOEt to remove the excess 2,2′-dithiobis(5-nitropyridine) (typically 6×2 mL or until no yellow colour was detected in the organic phase) and lyophilized to afford activated neamine **5**. Second, to a stirred solution of thioacetyl derivative **2** (2.4 mg, 3.6 μmol) in MeOH (1 mL) was added sodium methoxide (24 μL, 1 M in MeOH, 24 μmol) and the mixture stirred for 5 min at RT under argon. After evaporation *in vacuo*, the crude containing thiol amentantrone derivative **6** was dissolved in H_2O/ACN 8:2 (v/v) containing 0.1% TFA (8 mL) and added over the activated neamine **5**, and the mixture was stirred overnight under argon at RT. After purification by semipreparative reversed-phase HPLC (linear gradient from 0 to 80% B in 35 min; A, 0.1% TFA in H_2O; B, 0.1% TFA in ACN; R_t = 21 min) and lyophilization, the TFA salt of Amt$(Boc)_2$-Nea (**7**) was obtained as a blue solid (0.48 mg, yield 11%).

Compound **7** (400 nmol) and 1,3-di-Boc-2-trifluoromethylsulfonyl)guanidine (12.5 mg, 32 μmol) were dissolved in a 5:3 (v/v) mixture of MeOH and $CHCl_3$ (2 mL) under argon. Then, triethylamine (27 μL, 192 μmol) was added and the reaction mixture was stirred for 14 days at RT under Ar. A total of 360 mol equiv. of guanidinylating reagent and of 1680 mol equiv. of triethylamine was added over the entire reaction period. After evaporation *in vacuo*, the crude

was diluted with DCM (5 mL) and washed with a 10% aqueous solution of citric acid (3×1 mL) and with brine (3×1 mL). The organic phase was taken up and dried over anhydrous $MgSO_4$, filtered, and concentrated *in vacuo* to dryness. The crude product was dissolved in a 1:1 (v/v) mixture of TFA and DCM containing 2.5% of TIS (2 mL). After it was stirred at RT for 2 h under Ar, the mixture was diluted with toluene (2 mL) and evaporated *in vacuo*. After several coevaporations from toluene, the residue was dissolved in Milli-Q H_2O (5 mL) and lyophilized to provide a blue solid. Purification was carried out by analytical reversed-phase HPLC (linear gradient from 0 to 30% B in 35 min; A, 0.045% TFA in H_2O; B, 0.036% TFA in ACN), and the TFA salt of the desired product was obtained after lyophilisation (0.43 mg, yield 64% from **7**). ^{1}H NMR (600 MHz, D_2O) δ (ppm): 8.31 (2H, H_6+H_7 Amt, m), 7.86 (2H, H_5+H_8 Amt, m), 7.58 (2H, H_2+H_3 Amt, m), 5.58 (1H, $H_{1'}$, d, *J = 3.6 Hz*), 4.08 (1H, -S-CH_2-$\underline{CH_2}$-O-, m), 3.92 (2H, -NH-CH_2-$\underline{CH_2}$-OH, t, *J = 6.4 Hz*), 3.84 (4H, -NH-$\underline{CH_2}$-CH_2-NH-CH_2-, t, *J = 5.3 Hz*), 3.81 (1H, $H_{5'}$, m), 3.77 (1H, -S-CH_2-$\underline{CH_2}$-O-, m), 3.70 (2H, -NH-$\underline{CH_2}$-CH_2-S-, m), 3.68-3-58 (5H, $H_{2'}$, $H_{4'}$, H_4, H_5, H_6), 3.50-3.43 (5H, H_1, H_3, $H_{3'}$, -NH-CH_2-$\underline{CH_2}$-S-, m), 3.40 (2H, -NH-$\underline{CH_2}$-CH_2-OH, m), 3.20 (4H, -NH-CH_2-$\underline{CH_2}$-NH-CH_2-, m), 2.89 (2H, $H_{6'}$, m), 2.77 (2H, -S-$\underline{CH_2}$-CH_2-O-, m), 2.21 (1H, $H_{2,eq}$, m), 1.62 (1H, $H_{2,ax}$, m); HR-ESI MS, positive mode: *m/z* 977.4553 (calcd mass for $C_{40}H_{65}N_{16}O_9S_2$ $[M+H]^+$: 977.4562), *m/z* 489.2313 (calcd mass for $C_{40}H_{66}N_{16}O_9S_2$ $[M+2H]^{2+}$: 489.2320), *m/z* 326.4905 (calcd mass for $C_{40}H_{67}N_{16}O_9S_2$ $[M+3H]^{3+}$: 326.4906); analytical HPLC (linear gradient from 0 to 30% B in 30 min): R_t = 24.4 min.

Amt-Nea,Nea. First, the thiol function of the neamine derivative **4** (7 µmol) was activated by reaction with DTNP (27.2 mg, 87.5 µmol) in a 2:1 (v/v) mixture of THF/aqueous 0.1 % TFA (8 mL) under argon at RT for 17 h. After evaporation *in vacuo*, excess of DTNP was eliminated and the crude containing **5** was lyophilized. Second, to a stirred solution of the bis-thioester derivative

3 (1.4 mg, 1.9 μmol) in MeOH (1 mL) was added sodium methoxide (190 μL, 0.1 M in MeOH, 19 μmol) and the mixture stirred for 5 min at RT under argon. After evaporation *in vacuo*, the crude containing bis-thiol amentantrone derivative **8** was dissolved in H_2O/ACN 8:2 (v/v) containing 0.1% TFA (10 mL) and added over the activated neamine **5**, and the mixture was stirred for 5 days under argon at RT. After purification by analytical reversed-phase HPLC (linear gradient from 0 to 80% B in 35 min; A, 0.045% TFA in H_2O; B, 0.036% TFA in ACN; R_t = 18 min) and lyophilization, the TFA salt of Amt$(Boc)_2$-Nea,Nea was obtained. Finally, treatment with TFA/TIS/H_2O 95:2.5:2.5 (1 mL) for 1 h at RT afforded the TFA salt of Amt-Nea,Nea as a blue solid after HPLC purification (0.27 mg, yield 6%). ^{1}H NMR (600 MHz, D_2O) δ (ppm): 8.32 (2H, H_6+H_7 Amt, m), 7.89 (2H, H_5+H_8 Amt, m), 7.56 (2H, H_2+H_3 Amt, m), 5.62 (2H, $H_{1'}$, m), 4.15 (2H, -S-CH_2-$\underline{CH_2}$-O-, m), 3.98 (6H, $H_{5'}$, H_6, -S-CH_2-$\underline{CH_2}$-O-, m), 3.93 (4H, -NH-$\underline{CH_2}$-CH_2-NH-CH_2-, t, *J = 6.0 Hz*), 3.80 (2H, $H_{3'}$), 3.70 (4H, H_4, H_5, m), 3.61 (2H, $H_{4'}$, m), 3.46 (8H, -NH-CH_2-$\underline{CH_2}$-NH-$\underline{CH_2}$-, m), 3.40 (4H, $H_{6'}$, m), 3.20 (4H, H_1, H_3, m), 3.12 (2H, $H_{2'}$, m), 3.02 (4H, NH-CH_2-$\underline{CH_2}$-S-, t, *J = 6.8 Hz*), 2.92 (4H, -S-$\underline{CH_2}$-CH_2-O-, t, *J=6.3 Hz*), 2.23 (2H, $H_{2,eq}$, m), 1.56 (2H, $H_{2,ax}$, m); HR-ESI MS, positive mode: *m/z* 1205.5241 (calcd mass for $C_{50}H_{85}N_{12}O_{14}S_4$ $[M+H]^+$: 1205.5191), *m/z* 603.2642 (calcd mass for $C_{50}H_{86}N_{12}O_{14}S_4$ $[M+2H]^{2+}$: 603.2635), *m/z* 402.5122 (calcd mass for $C_{50}H_{87}N_{12}O_{14}S_4$ $[M+3H]^{3+}$: 402.5116); analytical HPLC (linear gradient from 0 to 30% B in 30 min): R_t = 22.7 min.

Amt-Nea,Azq. First, the thiol functions of neamine (1.5 μmol) and of azaquinolone monomers[10] (3 μmol) were activated with DTNP (5.8 mg, 18.8 μmol and 11.6 mg, 37.5 μmol, respectively) in a 2:1 (v/v) mixture of THF/aqueous 0.1 % TFA (1.5 and 2 mL, respectively) under argon at RT for 17 h. After evaporation *in vacuo*, excess of DTNP was eliminated and both activated derivatives were isolated by semipreparative reversed-phase HPLC (linear gradient from 0 to

80% B in 30 min; A, 0.1% TFA in H_2O; B, 0.1% TFA in ACN; R_t = 14.1 min for **5** and R_t = 17.9 min for **9**). Second, to a stirred solution of **3** (1 mg, 1.4 μmol) in MeOH (1 mL) was added sodium methoxide (275 μL, 0.1 M in MeOH, 27.5 μmol) and the mixture stirred for 5 min at RT under argon. After evaporation *in vacuo*, the crude containing derivative **8** was dissolved in H_2O/ACN 8:2 (v/v) containing 0.1% TFA (12 mL) and added over activated monomers **5** and **9**, and the mixture was stirred for 6 days under argon at RT. After purification by analytical reversed-phase HPLC (linear gradient from 0 to 80% B in 35 min; A, 0.045% TFA in H_2O; B, 0.036% TFA in ACN; R_t = 20.5 min) and lyophilization, the TFA salt of Amt$(Boc)_2$-Nea,Azq was obtained. Finally, treatment with TFA/TIS/H_2O 95:2.5:2.5 (1 mL) for 1 h at RT afforded the TFA salt of Amt-Nea,Azq as a blue solid after HPLC purification (0.21 mg, yield 8%). ^{1}H NMR (600 MHz, D_2O) δ (ppm): 7.95 (2H, H_6+H_7 Amt, m), 7.65 (2H, H_5+H_8 Amt, m), 7.57 (1H, H_5 Azq, d, *J = 7.8 Hz*), 7.53 (1H, H_4 Azq, d, *J = 9.5 Hz*), 7.33 (2H, H_2+H_3 Amt, m), 6.80 (1H, H_6 Azq, d, *J = 7.8 Hz*), 6.30 (1H, H_3 Azq, d, *J = 9.5 Hz*), 5.35 (1H, $H_{1'}$, m), 4.01 (2H, CH_2 Azq, s), 3.88-3.72 (7H, -S-CH_2-$\underline{CH_2}$-O-, -NH-$\underline{CH_2}$-CH_2-NH-, $H_{5'}$, m), 3.43-3.10 (16H, H_4, H_5, H_6, $H_{2'}$, $H_{3'}$, $H_{4'}$, -CO-NH-$\underline{CH_2}$-CH_2-CH_2-NH-, -NH-$\underline{CH_2}$-$\underline{CH_2}$-S-, m), 3.08-2.97 (4H, H_1, H_3, $H_{6'}$, m), 2.95 (2H, -CO-NH-CH_2-CH_2-$\underline{CH_2}$-NH-, t, *J = 7.9 Hz*), 2.90 (2H, -NH-CH_2-$\underline{CH_2}$-S-, t, *J = 6.3 Hz*), 2.85 (2H, -NH-CH_2-$\underline{CH_2}$-S-, t, *J = 6.3 Hz*), 2.81 (2H, -S-$\underline{CH_2}$-CH_2-CO-NH-, t, *J = 6.4 Hz*), 2.72 (2H, -S-$\underline{CH_2}$-CH_2-O-, m), 2.52 (2H, -S-CH_2-$\underline{CH_2}$-CO-NH-, t, *J = 6.4 Hz*), 2.02 (1H, $H_{2,eq}$, m), 1.79 (2H, -CO-NH-CH_2-$\underline{CH_2}$-CH_2-NH-, m), 1.38 (1H, $H_{2,ax}$, m); HR-ESI MS, positive mode: *m/z* 1143.4599 (calcd mass for $C_{51}H_{75}N_{12}O_{10}S_4$ $[M+H]^+$: 1143.4612), *m/z* 572.2334 (calcd mass for $C_{51}H_{76}N_{12}O_{10}S_4$ $[M+2H]^{2+}$: 572.2345), *m/z* 381.8250 (calcd mass for $C_{51}H_{77}N_{12}O_{10}S_4$ $[M+3H]^{3+}$: 381.8256); analytical HPLC (linear gradient from 5 to 35% B in 35 min): R_t = 22.8 min.

ASSOCIATED CONTENT

Supporting Information

Experimental procedures for the study of the interaction of the ligands with RNA. Reversed-phase HPLC traces and ^{1}H NMR spectra of the ligands. Representative UV melting curves of RNA-ligand complexes. This material is available free of charge via the Internet at http://pubs.acs.org.

AUTHOR INFORMATION

Corresponding Author

*E-mail: vmarchan@ub.edu.

ACKNOWLEDGEMENTS

The authors acknowledge Dr. M. Gairí from the Barcelona Scientific Park for NMR technical support, and Dr. I. Fernández and L. Ortiz from the facilities of the *Servei d'Espectrometria de Masses* of the University of Barcelona for MS support. This work was supported by funds from the Spanish *Ministerio de Ciencia e Innovación* (grant CTQ2010-21567-C02-01-02 and the RNAREG project, grant CSD2009-00080), the *Generalitat de Catalunya* (2009SGR-208 and the *Xarxa de Referència de Biotecnologia*) and the *Programa d'Intensificació de la Recerca* (Universitat de Barcelona). Gerard Artigas received a fellowship from the *Universitat de Barcelona.*

REFERENCES

(1) (a) Thomas, J. R.; Hergenrother, P. J. *Chem. Rev*. **2008**, *108*, 1171-1224. (b) Aboul-ela, F. *Future Med. Chem*. **2010**, *2*, 93-119. (c) Guan, L.; Disney, M. D. *ACS Chem. Biol*. **2012**, *7*, 73-86. (d) Guan, L.; Disney, M. D. *Angew. Chem. Int. Ed*. **2013**, *52*, 1462-1465. (e) Joly, J.-P.; Mata, G.; Eldin, P.; Briant, L.; Fontaine-Vive, F.; Duca, M.; Benhida, R. *Chem. Eur. J*., **2014**, *20*, 2071-2079. (f) Vo, D. D.; Staedel, C.; Zehnacker, L.; Benhida, R.; Darfeuille, F.; Duca, M. *ACS Chem. Biol*. **2014**, *9*, 711-721. (g) Blond, A.; Ennifar, E.; Tisne, C.; Micouin, L. *ChemMedChem* **2014**, *9*, 1982-1996. (h) Wong, C.-H.; Nguyen, L.; Peh, J.; Luu, L. M.; Sanchez, J. S.; Richardson, S. L.; Tuccinardi, T.; Tsoi, H.; Chan, W. Y.; Chan, H. Y. E.; Baranger, A. M.; Hergenrother, P. J.; Zimmerman, S. C. *J. Am. Chem. Soc*. **2014**, *136*, 6355-6361. (i) Warui, D. M.; Baranger, A. M. *J. Med. Chem*. **2012**, *55*, 4132-4141.

(2) (a) Gallego, J.; Varani, G. *Acc. Chem. Res*. **2001**, *34*, 836-843. (b) Tor, Y. *ChemBioChem*. **2003**, *4*, 998-1007. (c) Sharp, P. A. *Cell* **2009**, *136*, 577-580. (d) Georgianna, W. E.; Young, D. D. *Org. Biomol. Chem*. **2011**, *9*, 7969-7978. (e) Ofori, L. O.; Hoskins, J.; Nakamori, M.; Thornton, C. A.; Miller, B. L. *Nucleic Acids Res*. **2012**, *40*, 6380-6390. (f) Childs-Disney, J. L.; Parkesh, R.; Nakamori, M.; Thornton, C. A.; Disney, M. D. *ACS Chem. Biol*. **2012**, *7*, 1984-1993.

(3) (a) Overington, J. P.; Al-Lazikani, B.; Hopkins, A. L. *Nat. Rev. Drug Discovery*, **2006**, *5*, 993-996. (b) Schmidtke, P.; Barril, X. *J. Med. Chem*. **2010**, *53*, 5858-5867. (c) Fauman, E. B.; Rai, B. K.; Huang, E. S. *Curr. Opin. Chem. Biol*. **2011**, *15*, 463-468.

(4) (a) Chow, C. S.; Bogdan, F. M. *Chem. Rev*. **1997**, *97*, 1489-1513. (b) Zaman, G. J. R.; Michiels, P. J. A.; van Boeckel, C. A. A. *Drug Discov. Today* **2003**, *8*, 297-306.

(5) (a) Xia, T. *Curr. Opin. Chem. Biol*. **2008**, *12*, 604-611. (b) Tuccinardi, T. *Future Med. Chem*. **2011**, *3*, 723-733. (c) Bryson, D. I.; Zhang, W.; McLendon, P. M.; Reineke, T. M.; Santos, W. L.

ACS Chem. Biol. **2012**, *7*, 210-217. (d) Zhang, W.; Bryson, D. I.; Crumpton, J. B.; Wynn, J.; Santos, W. L. *Chem. Commun*. **2013**, *49*, 2436-2438

(6) (a) Shuker, S. B.; Hajduk, P. J.; Meadows, R. P.; Fesik, S. W. *Science* **1996**, *274*, 1531-1534. (b) Congreve, M.; Chessari, G.; Tisi, D.; Woodhead, A. J. *J. Med. Chem*. **2008**, *51*, 3661-3680. (c) Lee, M. M.; Childs-Disney, J. L.; Pushechnikov, A.; French, J. M.; Sobczak, K.; Thornton, C. A.; Disney, M. D. *J. Am. Chem. Soc*. **2009**, *131*, 17464-17472.

(7) (a) Donahue, C. P.; Ni, J.; Rozners, E.; Glicksman, M. A.; Wolfe, M. S. *J. Biomol. Screening* **2007**, *12*, 789-799. (b) Zheng, S.; Chen, Y.; Donahue, C. P.; Wolfe, M. S.; Varani, G. *Chem. Biol*. **2009**, *16*, 557-566. (c) Liu, Y.; Peacey, E.; Dickson, J.; Donahue, C. P.; Zheng, S.; Varani, G.; Wolfe, M. S. *J. Med. Chem*. **2009**, *52*, 6523-6526. (d) Liu, Y.; Rodriguez, L.; Wolfe, M. S. *Bioorg. Chem.* **2014**, *54*, 7-11.

(8) (a) Noble, W.; Pooler, A. M.; Hanger, D. P. *Expert Opin. Drug. Discov*. **2011**, *6*, 797-810. (b) Varani, L.; Hasegawa, M.; Spillantini, M. G.; Smith, M. J.; Murrell, J. R.; Ghetti, B.; Klug, A.; Goedert, M.; Varani, G. *Proc. Natl. Acad. Sci. U. S. A*. **1999**, *96*, 8229-8234. (c) Donahue, C. P.; Muratore, C.; Wu, J. Y.; Kosik, K. S.; Wolfe, M. S. *J. Biol. Chem*. **2006**, *281*, 23302-23306. (d) Spillantini, M. G.; Murrell, J. R.; Goedert, M.; Farlow, M. R.; Klug, A. *Proc. Natl. Acad. Sci. U.S.A*. **1998**, *95*, 7737-7741. (e) Liu, F.; Gong, C. X. *Mol. Neurodegener*. **2008**, 3:8; (f) Wolfe, M. S. *J. Biol. Chem*. **2009**, *284*, 6021-6025. (g) Niblock, M.; Gallo, J.-M. *Biochem. Soc. Trans*. **2012**, *40*, 677-680.

(9) Stelzer, A. C.; Frank, A. T.; Kratz, J. D.; Swanson, M. D.; Gonzalez-Hernandez, M. J.; Lee, J.; Andricioaei, I.; Markovitz, D. M.; Al-Hashimi, H. M. *Nat. Chem. Biol*. **2011**, *7*, 553-559.

(10) (a) López-Senín, P.; Gómez-Pinto, I.; Grandas, A.; Marchán, V. *Chem. Eur. J*. **2011**, *17*, 1946-1953. (b) López-Senín, P.; Artigas, G.; Marchán, V. *Org. Biomol. Chem*. **2012**, *10*, 9243-254.

(11) (a) Gianoncelli, A.; Basili, S.; Scalabrin, M.; Sosic, A.; Moro, S.; Zagotto, G.; Palumbo, M.; Gresh, N.; Gatto, B. *ChemMedChem* **2010**, *5*, 1080-1091. (b) Skladanowski, A.; Konopa, J. *British J. Cancer* **2000**, *82*, 1300-1304.

(12) Artigas, G.; López-Senín, P.; González, C.; Escaja, N.; Marchán, V. *Org. Biomol. Chem.* **2015**, *13*, 452-464.

(13) (a) Kirk, S. R.; Luedtke, N. W.; Tor, Y. *J. Am. Chem. Soc*. **2000**, *122*, 980-981. (b) Zhang, J.; Umemoto, S.; Nakatani, K. *J. Am. Chem. Soc*. **2010**, *132*, 3660-3661. (c) Tran, T.; Disney, M. D. *Nat. Commun*. **2012**, *3*, 1-9.

(14) Hagihara, S.; Kumasawa, H.; Goto, Y.; Hayashi, G.; Kobori, A.; Saito, I.; Nakatani, K. *Nucleic Acids Res*. **2004**, *32*, 278-286.

(15) Artigas, G.; Marchán, V. *J. Org. Chem*. **2013**, *78*, 10666-10677.

(16) Rabanal, F.; DeGrado, W. F.; Dutton, D. L. *Tetrahedron Lett*. **1996**, *37*, 1347-1350.

(17) (a) Luedtke, N. W.; Baker, T. J.; Goodman, M.; Tor, Y. *J. Am. Chem. Soc*. **2000**, *122*, 12035-12036. (b) Luedtke, N. W.; Carmichael, P.; Tor, Y. *J. Am. Chem. Soc*. **2003**, *125*, 12374-12375. (c) Grau-Campistany, A.; Massaguer, A.; Carrion-Salip, D.; Barragán, F.; Artigas, G.; López-Senín, P.; Moreno, V.; Marchán, V. *Mol. Pharmaceutics* **2013**, *10*, 1964-1976.

(18) Blakeley, B. D.; DePorter, S. M.; Mohan, U.; Burai, R.; Tolbert, B. S.; McNaughton, B. R. *Tetrahedron* **2012**, *68*, 8837-8855.

(19) (a) Moumné, R.; Catala, M.; Larue, V.; Micouin, L.; Tisné, C. *Biochimie* **2012**, *94*, 1607–1619. (b) Lombes, T.; Moumne, R.; Larue, V.; Prost, E.; Catala, M.; Lecourt, T.; Dardel, F.; Micouin, L.; Tisne, C. *Angew. Chem. Int. Ed*. **2012**, *51*, 9530-9534.